University of Reading

Engineering of a novel amphibian skin peptide isolated from Agua Rica Leaf Frog (Callimedusa ecuatoriana) into active antimicrobial agents

Article

Published Version

Creative Commons: Attribution 4.0 (CC-BY)

Open Access

Bonilla-Jiménez, S., Espinosa de los Monteros-Silva, N. ORCID: https://orcid.org/0000-0002-7503-1165, Morán-Marcillo, G. ORCID: https://orcid.org/0000-0003-3233-6572, Bermúdez-Puga, S. ORCID: https://orcid.org/0000-0002-7356-8655, Terán-Valdez, A. ORCID: https://orcid.org/0009-0001-2489-7313, Almeida, J. R. ORCID: https://orcid.org/0000-0002-4637-4468 and Proaño-Bolaños, C. ORCID: https://orcid.org/0000-0001-9279-1038 (2025) Engineering of a novel amphibian skin peptide isolated from Agua Rica Leaf Frog (Callimedusa ecuatoriana) into active antimicrobial agents. Antibiotics, 14 (12). 1186. ISSN 2079-6382 doi: 10.3390/antibiotics14121186 Available at https://centaur.reading.ac.uk/127312/

It is advisable to refer to the publisher's version if you intend to cite from the work. See Guidance on citing.

To link to this article DOI: http://dx.doi.org/10.3390/antibiotics14121186

University of Reading

Publisher: MDPI

All outputs in CentAUR are protected by Intellectual Property Rights law, including copyright law. Copyright and IPR is retained by the creators or other copyright holders. Terms and conditions for use of this material are defined in the End User Agreement.

www.reading.ac.uk/centaur

CentAUR

Central Archive at the University of Reading

Reading's research outputs online

antibiotics

MDPI

Article

Engineering of a Novel Amphibian Skin Peptide Isolated from Agua Rica Leaf Frog (*Callimedusa ecuatoriana*) into Active Antimicrobial Agents

Stefanny Bonilla-Jiménez [1,†], Nina Espinosa de los Monteros-Silva [2,†], Giovanna Morán-Marcillo [2], Sebastián Bermúdez-Puga [1,3], Andrea Terán-Valdez [4], José R. Almeida [1,5] and Carolina Proaño-Bolaños [1,2,*]

1 Biomolecules Discovery Group, Universidad Regional Amazónica Ikiam, km 7 ½ vía Muyuna, Tena 150150, Ecuador; stefanny.bonilla@epn.edu.ec (S.B.-J.); sebastianbermudez@usp.br (S.B.-P.); rafael.dealmeida@ikiam.edu.ec (J.R.A.)
2 Laboratory of Molecular Biology and Biochemistry, Universidad Regional Amazónica Ikiam, km 7 ½ vía Muyuna, Tena 150150, Ecuador; nina.espinosadelosmonteros@ikiam.edu.ec (N.E.d.l.M.-S.); giovanna.moran@ikiam.edu.ec (G.M.-M.)
3 Laboratory of Microbial Biomolecules, Department of Biochemical and Pharmaceutical Technology, University of São Paulo, São Paulo 05508-000, Brazil
4 Centro Jambatu de Investigación y Conservación de Anfibios, Fundación Jambatu, San Rafael, Quito 171102, Ecuador
5 School of Pharmacy, University of Reading, Reading RG6 6UB, UK
* Correspondence: carolina.proano@ikiam.edu.ec
† These authors contributed equally to this work.

Abstract

Background/Objectives: The increasing antimicrobial resistance is a current human health threat, which has stimulated research on new biologically active molecules against infections caused by microorganisms resistant to conventional therapies. Antimicrobial peptides (AMPs) from amphibian skin secretions have generated great interest in tackling this problem due to their antibacterial, antifungal, antiprotozoal, wound-healing, and even anticancer properties. In Ecuador, there are still unexplored endemic amphibian species as a source of new AMPs, such as *Callimedusa ecuatoriana*. In this study, we report a novel peptide derived from the skin secretion of *Callimedusa ecuatoriana* identified by molecular cloning of the mRNA precursor. The functional analysis demonstrated that it lacks antimicrobial activity due to its alpha-helix kink structure. **Methods**: Inspired by the native structure of PTR-CE1, we designed and synthesized two analogs (PTR-CE1a and PTR-CE1b) to adopt a complete α-helix secondary structure, a conformation often associated with antimicrobial activity. In silico tools were used to predict the peptide activity, which was confirmed by experimental findings. **Results**: Both analogs displayed higher activity than the native peptide, even against the ampicillin-resistant bacterial strain. While PTR-CE1b showed Minimum Inhibitory Concentration (MIC) values of 26.62–212.99 µM and 24.36% of hemolytic activity at 26.62 µM, PTR-CE1a displayed a more potent broad-spectrum activity against all the microorganisms, with MIC values of 3.02–12.06 µM and hemolytic activity of 7.5% at 3.02 µM. **Conclusions**: This study demonstrates the importance of the α-helix structure for antimicrobial activity in *C. ecuatoriana* PTR-CE1 analogs and highlights the potential of unexplored biological and molecular diversity in endemic species of Ecuador to provide novel templates for peptide design.

Keywords: toxicity; synthetic antimicrobial peptides; amphibian skin secretion peptides; proline alpha-helix kink

check for updates

Academic Editor: Fernando Albericio

Received: 30 October 2025
Revised: 17 November 2025
Accepted: 19 November 2025
Published: 21 November 2025

Citation: Bonilla-Jiménez, S.; Espinosa de los Monteros-Silva, N.; Morán-Marcillo, G.; Bermúdez-Puga, S.; Terán-Valdez, A.; Almeida, J.R.; Proaño-Bolaños, C. Engineering of a Novel Amphibian Skin Peptide Isolated from Agua Rica Leaf Frog (*Callimedusa ecuatoriana*) into Active Antimicrobial Agents. *Antibiotics* **2025**, *14*, 1186. https://doi.org/10.3390/antibiotics14121186

Copyright: © 2025 by the authors. Licensee MDPI, Basel, Switzerland. This article is an open access article distributed under the terms and conditions of the Creative Commons Attribution (CC BY) license (https://creativecommons.org/licenses/by/4.0/).

1. Introduction

Antimicrobial resistance (AMR) has emerged as a critical global public health problem [1]. The increase in multidrug-resistant bacteria severely limits our ability to treat infections, leading to increased mortality, particularly in hospital settings. Alarmingly, projections suggest AMR could become the leading cause of death by 2050, claiming over 10 million lives annually [2]. For this reason, there is an urgent need to develop innovative approaches to confront this problem [3].

In this context, amphibian skin secretions have gained attention in antibiotic discovery programs as valuable sources of novel antimicrobial agents. These secretions are a rich natural reservoir of novel antimicrobial peptides (AMPs), which constitute a key component of their innate defense system against predators and pathogens [4,5]. Beyond their antimicrobial properties, these bioactive molecules demonstrate a broad range of therapeutic activities, including diverse properties such as analgesic [6], anti-inflammatory [7], antidiabetic [8], anticancer [9,10], wound-healing [11,12], antioxidant [13], hemostasis effectors [14], and antimicrobial [12,15,16]. This illustrates the potential of peptides as versatile candidates for drug discovery and therapeutic development.

Noticeably, amphibians contribute nearly 60% of all antimicrobial peptides (AMPs) cataloged in the Antimicrobial Peptide Database (APD; ~1900 of 3306 entries) [5,17] (APD, https://aps.unmc.edu, accessed on 1 December 2024), underscoring their pharmaceutical potential [18]. Among amphibian families, Phyllomedusidae exhibit exceptional AMP diversity, comprising eight genera (*Agalychnis*, *Callimedusa*, *Cruziohyla*, *Hylomantis*, *Phasmahyla*, *Phrynomedusa*, *Phyllomedusa*, and *Pithecopus*). While *Phyllomedusa* has been extensively studied (>110 described AMPs) [5,19], *Callimedusa* remains largely unexplored, with only seven reported AMPs [20–24]. This study focuses on *Callimedusa ecuatoriana*, an Ecuadorian endemic species [25], to expand our understanding of this underexplored resource.

Amphibian AMPs represent compelling candidates against drug-resistant pathogens due to their unique mechanism of action [3,26]. Unlike conventional antibiotics, AMPs typically disrupt plasma membrane integrity or target intracellular components and exhibit low propensity for resistance development [27,28]. However, clinical applications face challenges such as limited bioactivity, host toxicity, and proteolytic instability [29–33]. Peptide engineering emerges as a powerful solution to these limitations, enabling the design of synthetic analogs with enhanced antimicrobial properties and reduced toxicity [34–36].

Here, we characterize PTR-CE1, a novel Picturin peptide isolated from *C. ecuatoriana* skin secretions. Using this natural peptide as a template, we designed two α-helix-stabilized analogs to investigate how secondary structure influences antimicrobial activity.

2. Results

2.1. Molecular Cloning of cDNA Encoding PTR-CE1 Precursor

One nucleotide sequence encoding a propeptide was identified from the skin secretion of *C. ecuatoriana* (Figure 1). The translated open-reading frame consisted of 74 amino acids composed of three domains: (1) the signal peptide of 22 amino acids in the N-terminal region, (2) a 27-residue acidic spacer domain containing the KR propeptide processing site, and (3) a 25-mer mature peptide.

The nucleotide sequences and translated ORF amino acid sequences were analyzed using NCBI-BLAST (https://blast.ncbi.nlm.nih.gov/Blast.cgi, accessed on 15 March 2024), revealing a 76.85% similarity with pro-peptide pictuseptin-2 precursor (GeneBank: MW118451.1), 88.49% similarity with pro-peptide boanin-3 (GeneBank: ON703100.1), and 96–98% similarity with pro-peptides from picturin 1, picturin 2, and picturin 3 (GeneBank: MN652613.1, MN652614.1, and MN652615.1, respectively) (Table 1), all isolated from the skin secretion of *Boana picturata* [37]. The alignment with picturins was obtained with more than 93% of

query coverage, especially focusing on the signal region and acidic spacer region. These findings suggest that the novel peptide belongs to the picturin family (PTR). Consequently, it was named picturin-CE1 (PTR-CE1) to reflect its origin in *C. ecuatoriana*. The peptide was chemically synthesized for evaluation of its antimicrobial and hemolytic activities.

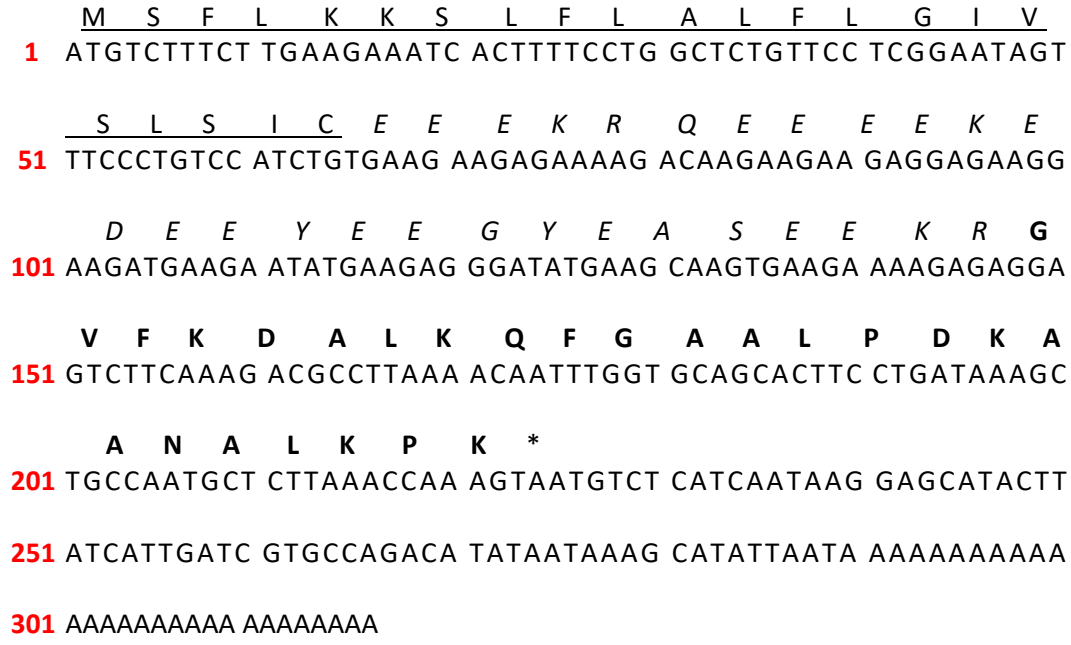

Figure 1. Nucleotide and translated open-reading frame (ORF) amino acid sequence of the sense strand of cloned cDNA encoding PTR-CE1 (OQ438429). Underlined: putative signal peptide; italic: acidic spacer; bold: mature peptide; asterisks: stop codon.

2.2. Peptide Design, Predicted Physicochemical Characteristics, and 3D Models

PTR-CE1 is a 25-mer peptide with a hydrophobicity of 0.236 with a net charge of +3 (Table 2). Compared with other picturin members, PTR-CE1 differs from PTR-2 by a single substitution (Pro15 → Leu) and from PTR-3 by two substitutions (Pro15 → Leu and Lys17 → Gln) (Table 2). These positions include a helix-breaking residue (Pro15) and a charge-altering substitution at position 17, suggesting these differences may influence bioactivity. Previous antimicrobial results demonstrated that PTR-1, PTR-2, and PTR-3 inhibited Gram-positive and Gram-negative bacteria [37].

Based on this information, two analogs were designed using the natural AMP identified in this study to investigate the roles of proline and to increase net charge. PTR-CE1a incorporates four substitutions (Asp5 → Lys, Pro15 → Leu, Asp16 → Arg, and Lys17 → Leu), increasing net charge and restoring the continuous alpha-helix (Table 2). PTR-CE1b is a 23-mer peptide, lacking both proline residues to restore continuous helicity (Table 2). These modifications alter hydrophobicity, peptide length, and net charge, parameters known to influence antimicrobial potency and selectivity. For example, PTR-CE1a and PTR-CE1b have a net charge of +7 and +4, respectively, while the net charge of the native peptide is +3. Both analogs, PTR-CE1a and PTR-CE1b, were C-terminally amidated to reduce proteolytic susceptibility and increase the net charge.

The helical wheel plots demonstrated that peptides are amphipathic (Figure 2). PTR-CE1a exhibited a more pronounced hydrophobic face compared to PTR-CE1 and PTR-CE1b. The three-dimensional structure models obtained using I-TASSER revealed that PTR-CE1a and PTR-CE1b form a single α-helix, whereas PTR-CE1 adopts two α-helices in its structure due to the presence of a proline residue.

Table 1. Domain structure comparison of PTR-CE1 with other similar peptide precursors.

Peptide	Signal Peptide																					
	1																					
Picturin-CE1	M	S	F	L	K	K	S	L	F	L	A	L	F	L	G	I	V	S	L	S	I	C
Picturin-2	M	S	F	L	K	K	S	L	F	L	V	L	F	L	G	I	V	S	L	S	I	C
Picturin-3	-	-	-	-	-	K	S	L	F	L	V	L	F	L	G	I	V	S	L	S	I	C
Picturin-1	-	-	-	-	-	-	S	L	F	L	V	L	F	L	G	I	V	S	L	S	I	C
Boanin-3	M	T	F	G	K	K	S	L	F	L	V	L	F	L	G	M	V	S	L	S	I	C
Pictuseptin-2	M	S	F	L	K	K	S	L	F	L	V	L	F	L	G	I	V	S	L	S	I	C

Peptide	Acidic spacer																												
	23																												
Picturin-CE1	E	E	E	K	R	-	-	Q	E	E	E	E	K	E	D	E	E	Y	E	E	G	Y	E	A	S	E	E	K	R
Picturin-2	E	E	E	K	R	-	-	Q	E	E	E	E	K	E	D	E	E	Y	E	E	G	Y	E	A	S	E	E	K	R
Picturin-3	E	E	E	K	R	-	-	Q	E	E	E	E	K	E	D	E	E	Y	E	E	G	Y	E	A	S	E	E	K	R
Picturin-1	E	E	E	K	R	-	-	Q	E	E	E	E	K	E	D	E	E	Y	E	E	G	Y	E	A	S	E	E	K	R
Boanin-3	Q	D	E	K	R	-	E	E	E	E	E	E	K	E	E	E	E	Y	E	E	G	N	E	E	H	K	E	K	R
Pictuseptin-2	E	E	E	K	K	Q	A	E	E	E	E	E	K	Q	E	E	Q	Y	D	Q	E	N	E	E	Y	K	E	K	R

Peptide	Mature peptide																														Accession number
	52																														
Picturin-CE1	-	-	-	G	V	F	K	D	A	L	K	Q	F	G	A	A	L	[illegible]	D	K	A	A	N	A	L	K	P	K	*		OQ438429.1
Picturin-2	-	-	-	G	V	F	K	D	A	L	K	Q	F	G	A	A	L	L	D	K	A	A	N	A	L	K	P	K	*		MN652614.1
Picturin-3	-	-	-	G	V	F	K	D	A	L	K	Q	F	G	A	A	L	L	D	Q	A	A	N	A	L	K	P	K	*		MN652615.1
Picturin-1	-	-	-	G	V	F	K	D	A	L	K	Q	L	G	A	A	L	L	D	K	A	A	N	A	L	K	P	K	*		MN652613.1
Boanin-3	-	F	L	G	A	L	F	A	I	G	K	A	I	G	K	A	I	L	P	L	A	V	K	A	F	N	P	Q	H	*	ON703100.1
Pictuseptin-2	G	F	L	D	T	L	K	N	I	G	K	T	V	G	-	-	-	-	G	I	A	L	N	V	L	T	G	*			MW118451.1

Light gray: Conserved sites in all sequences. Dark gray: Similar sites only in the mature peptide region. Black: Unique amino acid in mature peptide region of PTR-CE1. *: Stop codon.

Table 2. Physicochemical characteristics of PTR, PTR-CE1, and their analogs.

Peptide	Sequence	#Aas	Alpha Helix %	Hydrophobicity <H>	Hydrophobic Moment <mH>	Net Charge Z	Theoretical Mass	Ref.
PTR-CE1	h h h h h h h h h h h h h c c h h h h h h h c t t G V F K D A L K Q F G A A L P D K A A N A L K P K	25	80	0.236	0.506	3	2599.07	
PTR-CE1a	h h h h h h h h h h h h h h h h h h h h h h h c t t G V F K K A L K Q F G A A L L R L A A N A L K P K a	25	88	0.364	0.462	7	2653.30	
PTR-CE1b	h h h h h h h h h h h h h h h h h h h h h h h h h h G V F K D A L K Q F G A A L D K A A N A L K K a	23	100	0.193	0.468	4	2403.85	
PTR-1	h h h h h h h h h h h h h h h h h h h h h h h c t t G V F K D A L K Q L G A A L L D K A A N A L K P K	25	88	0.271	0.306	3	2581.10	[37]
PTR-2	h h h h h h h h h h h h h h h h h h h h h h h c t t G V F K D A L K Q F G A A L L D K A A N A L K P K	25	88	0.275	0.309	3	2615.12	[37]
PTR-3	h h h h h h h h h h h h h h h h h h h h h h h c t t G V F K D A L K Q F G A A L L D Q A A N A L K P K	25	88	0.306	0.326	2	2615.07	[37]

a = amidation, h = alpha helix, t = beta turn, c = random coil.

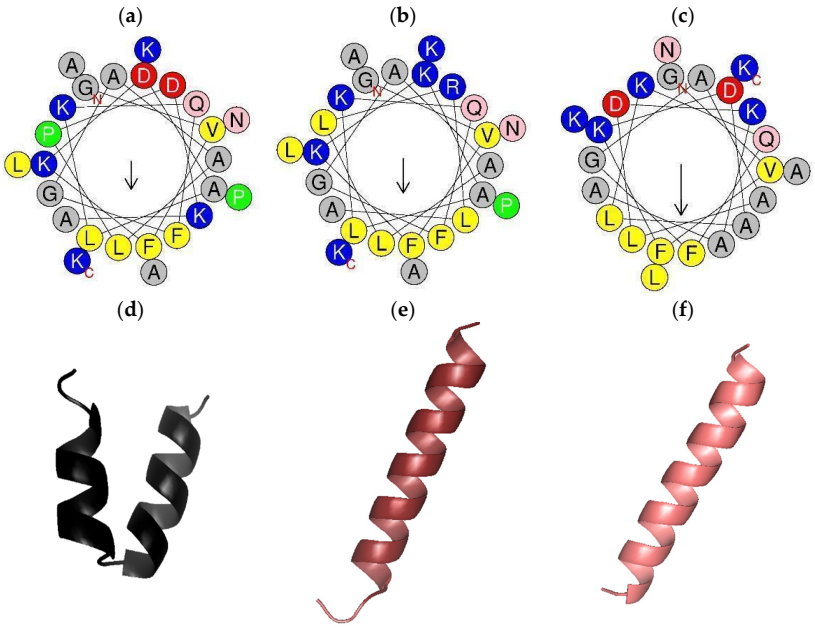

Figure 2. Helical wheel plots and 3D models of PTR-CE1 and their analogs. (**a**) Helical wheel plot of (**a**) PTR-CE1, (**b**) PTR-CE1a, (**c**) PTR-CE1b, and predicted 3D models of (**d**) PTR-CE1, (**e**) PTR-CE1a, (**f**) PTR-CE1b. Residue color code in the helical model: yellow = hydrophobic non-polar, gray = uncharged, blue = polar, red = acid, pink = unladen polar, and green = Pro. Arrows detail a hydrophobic face.

2.3. In Silico Bioactivity Predictions and Molecular Docking

In silico results showed that PTR-CE1 and its analogs probably have antimicrobial effects (Table 3). Furthermore, HemoPI-2 and ToxinPred analyses predicted that all peptides could induce low hemolysis and are not toxic (Table 3).

Table 3. In silico screening of antimicrobial effect, hemolytic activity, and toxicity of PTR-CE1 and its analogs.

Peptide	CAMPR3 (SVM *)	HemoPI-2	ToxinPred
	Antimicrobial		
PTR-CE1	0.915	0.52	Non-toxin
PTR-CE1a	0.994	0.58	Non-toxin
PTR-CE1b	0.908	0.54	Non-toxin

* SVM = Support Vector Machine.

Molecular docking analysis revealed a favorable interaction and affinity between the peptide analogs and the bacterial membrane (Figure 3). PTR-CE1a exhibited a score of −8.4 kcal/mol, and PTR-CE1b showed a score of −4.7 kcal/mol. Considering these in silico data, the peptide analogs were synthesized, and the in vitro bioactivity was evaluated.

2.4. Synthesis and Characterization of Peptides

Chromatography profiles showed that all crude synthetic peptides had >80% purity, and the mass spectrum corroborated the peptide identity (Figure 4), based on the theoretical mass (Table 2).

2.5. Antimicrobial Activity of PTR-CE1 and Its Analogs

The antimicrobial activity of the three peptides was evaluated against *Escherichia coli* ATCC 25922, *Staphylococcus aureus* ATCC 29213, *Candida albicans* ATCC 10231, and the ampicillin-resistant strains of *Bacillus subtilis*, *Klebsiella pneumoniae*, and *Pseudomonas aeruginosa*. The native peptide, PTR-CE1, showed no antimicrobial or antifungal activity

(Table 4), contrary to in silico predictions. This result highlights the importance of experimental validation to confirm the predicted bioactivity of peptides. On the other hand, the peptide analogs displayed broad-spectrum antimicrobial properties (Table 4) in agreement with the in silico prediction (Table 3). PTR-CE1a emerged as the most potent analog, exhibiting growth inhibition against all tested microorganisms (MIC = 3.02–12.06 μM), including ampicillin-resistant strains. Furthermore, this peptide displayed broad-spectrum antimicrobial activity against Gram-positive bacteria, Gram-negative bacteria, and yeast.

PTR-CE1b showed antimicrobial activity against all bacteria tested except *S. aureus*, including ampicillin-resistant isolates of *E. coli*, *K. pneumoniae*, and *B. subtilis* (MIC = 26.62–53.25 μM) (Table 4). In contrast, its activity against *C. albicans* was markedly weaker (MIC = 212.99 μM).

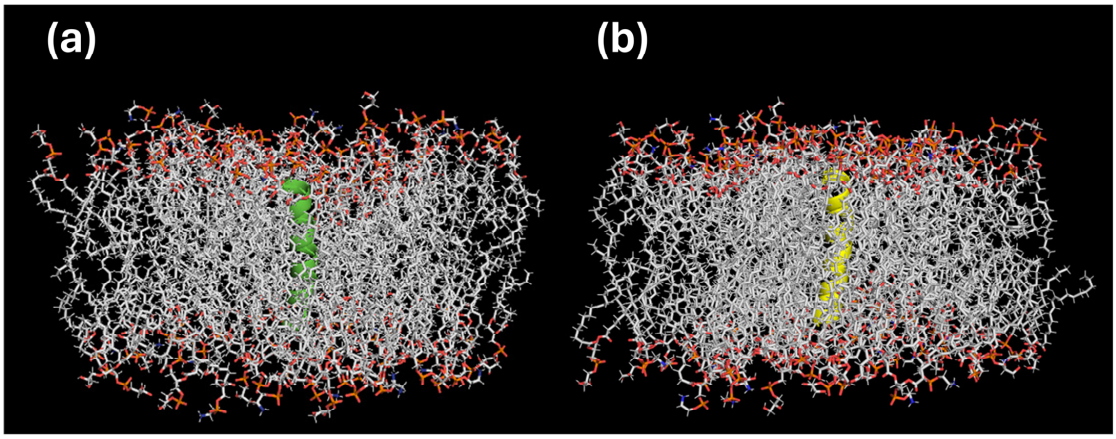

Figure 3. Docking interactions of (**a**) PTR-CE1a (green color) and (**b**) PTR-CE1b (yellow color) with the bacterial cell membrane.

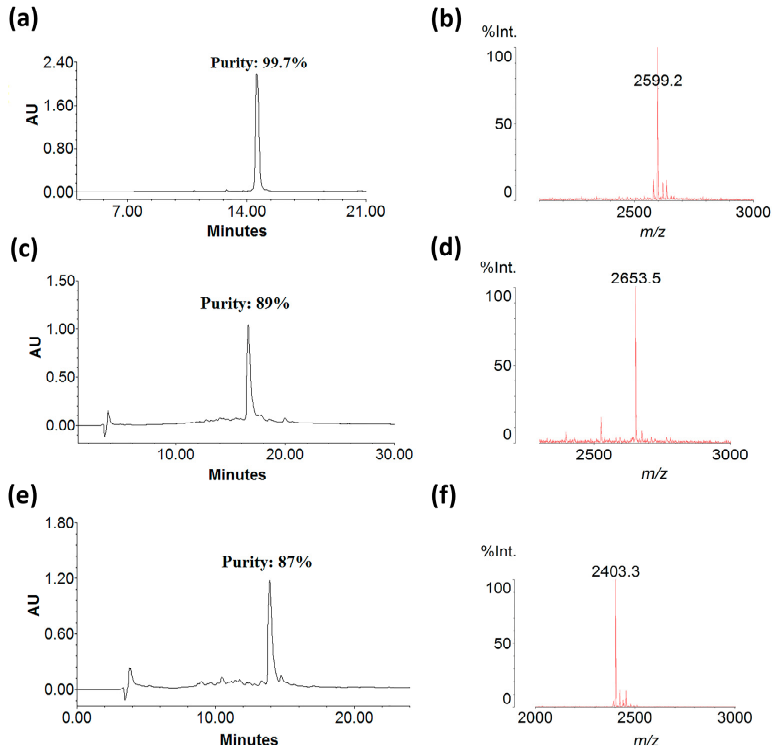

Figure 4. Relative purity and mass spectra of peptides obtained by RP-HPLC and MALDI TOF MS. (**a**) PTR-CE1 purity (99.7%). (**b**) Monoisotopic mass/charge of PTR-CE1 (2599.2 Da). (**c**) PTR-CE1a purity (89%). (**d**) Monoisotopic mass/charge of PTR-CE1a (2653.5 Da). (**e**) PTR-CE1b purity of PTR-CE1b (87%). (**f**) Monoisotopic mass/charge of PTR-CE1b (2403.3 Da).

Table 4. Minimum inhibitory concentration (MIC) and minimum bactericidal concentration (MBC) of PTR-CE1 and its analogs.

	MIC μM (mg/L)						MBC μM (mg/L)						Ref.
Synthetic Peptide	***E. coli*** **25922**	***S. aureus*** **25923**	***C. albicans***	***K. pneumoniae*** **(AMP-RES) Clinical Isolate**	***P. aeruginosa*** **(AMP-RES) Clinical Isolate**	***Bacillus subtilis*** **(AMP-RES) Clinical Isolate**	***E. coli*** **25922**	***S. aureus*** **25923**	***C. albicans***	***K. pneumoniae*** **(AMP-RES) Clinical Isolate**	***P. aeruginosa*** **(AMP-RES) Clinical Isolate**	***Bacillus subtilis*** **(AMP-RES) Clinical Isolate**	
Picturin-CE1	>196.99 (>512)	>196.99 (>512)	>196.99 (>512)	>196.99 (>512)	>196.99 (>512)	>196.99 (>512)	>196.99 (>512)	>196.99 (>512)	>196.99 (>512)	>196.99 (>512)	>196.99 (>512)	>196.99 (>512)	
Picturin-CE1a	3.02 (8)	6.03 (16)	12.06 (32)	6.03 (16)	12.06 (32)	3.02 (8)	6.03 (16)	12.06 (32)	>192.96 (>512)	12.06 (32)	48.24 (128)	24.12 (64)	
Picturin-CE1b	53.25 (128)	>212.99 (>512)	212.99 (512)	53.25 (128)	26.62 (64)	26.62 (64)	106.49 (256)	>212.99 (>512)	>212.99 (>512)	106.49 (256)	>212.99 (>512)	53.25 (128)	
* Picturin-1	24.80 (64)	198.37 (512)	>198.37 (>512)	ND	ND	ND	>198.37 (>512)	>198.37 (>512)	>198.37 (>512)	ND	ND	ND	[37]
* Picturin-2	48.95 (128)	>195.79 (>512)	>195.79 (>512)	ND	ND	ND	48.95 (128)	>195.79 (>512)	>195.79 (>512)	ND	ND	ND	[37]
* Picturin-3	48.98 (128)	97.95 (256)	>195.91 (>512)	ND	ND	ND	48.98 (128)	>195.91 (>512)	>195.91 (>512)	ND	ND	ND	[37]
* Pseudin-2 [Lys3,10,14,21]	5	20	ND	ND	ND	ND	ND	ND	ND	ND	ND	ND	[38]
* Hylin a1-2A	16	2	ND	ND	ND	ND	ND	ND	ND	ND	ND	ND	[39]
* Brevinin-1BYa [Ser18,Ser24]	20	ND	ND	ND	ND	ND	ND	ND	ND	ND	ND	ND	[40]
* Alysterin-2a	ND	64	64	ND	ND	ND	ND	ND	ND	ND	ND	ND	[41]
* Kassinatuerin-1 [Lys7,Lys18,Lys19]	6.25	6.25	25	ND	ND	ND	ND	ND	ND	ND	ND	ND	[42]
* Brevinin-2Ob	4	9	40										
* Ampicillin	46	<11	ND	ND	ND	ND	ND	ND	ND	ND	ND	ND	[12]
* Fluconazole	ND	ND	209	ND	ND	ND	ND	ND	ND	ND	ND	ND	[16]

ND = No data. * MIC values of analog peptides from amphibian skin secretion of other species and commercial drugs were added for comparison.

2.6. Hemolytic Activity of Peptides

PTR-CE1 exhibited only 2.64% of hemolytic activity at the highest tested peptide concentration (196.99 µM). In contrast, both analogs displayed higher hemolytic activity than the native peptide. PTR-CE1a showed 7.5–39.1% hemolytic activity at the MICs against the tested pathogens (MIC = 3.02–12.06 µM), whereas PTR-CE1b induced 24.36–40.64% hemolytic activity at the MIC (26.62–212.99 µM) (Figure 5).

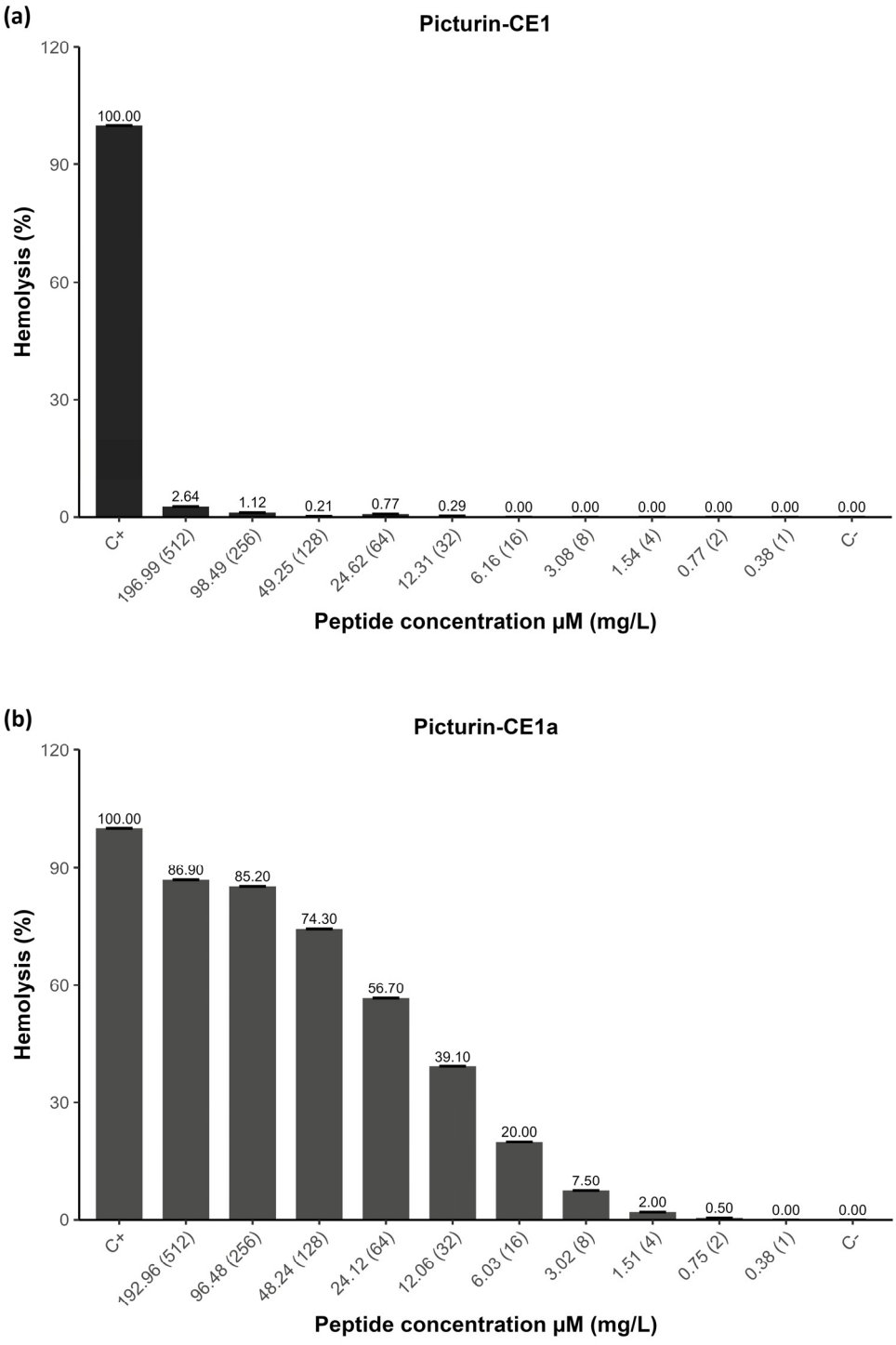

Figure 5. *Cont.*

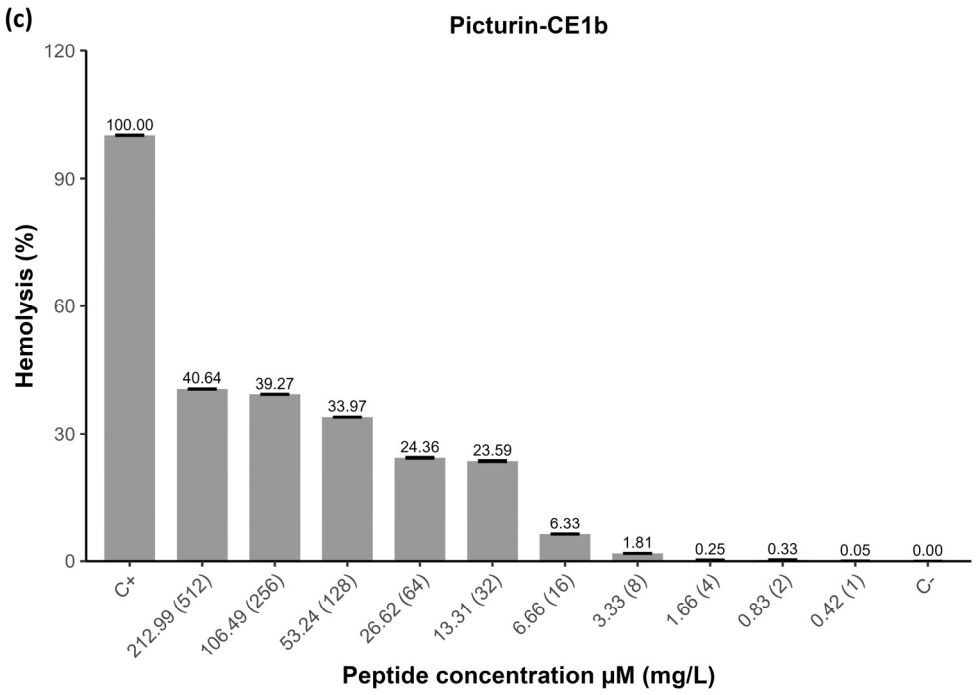

Figure 5. Hemolytic activity of (**a**) PTR-CE1, (**b**) PTR-CE1a, and (**c**) PTR-CE1b. PBS 1X was used as a negative control, and Triton X-100 (2% *v*/*v*) was used as a positive control.

3. Discussion

Several studies have shown the abundance of antimicrobial peptides (AMPs) in frog skin secretions [5,8,43]. However, hundreds of species remain unstudied, especially in megadiverse countries like Ecuador [44]. In this study, molecular cloning identified a novel peptide precursor (PTR-CE1) from the skin secretion of the endemic frog *Callimedusa ecuatoriana*. The signal peptide and the acidic spacer of the PTR-CE1 precursor showed a high similarity with those of picturins [37], a peptide family previously described in *Boana picturata* (Table 1). In fact, the mature peptide was 92–96% similar to picturin peptides, justifying its inclusion in this family. The mature PTR-CE1 peptide is composed of 25 amino acid residues and is the first skin secretion peptide reported from this endemic Ecuadorian frog species.

All previously reported members of the picturin family have antibacterial properties, such as PTR-1, PTR-2, and PTR-3 [37]. PTR-1 showed the highest activity against *E. coli* (MIC = 24.80 μM) and *S. aureus* (MIC = 198.37 μM). However, PTR-CE1 did not inhibit the growth of the tested bacteria. PTR-1 and PTR-CE1 share some characteristics, such as a cationic charge (+3) and similar hydrophobicity values (0.236–0.271). However, their primary sequence differs in the amino acid composition: at position 10 (Leu/Phe) and at position 15 (Leu/Pro). Likewise, PTR-2 has an amino acid substitution at position 15 (Leu/Pro) compared to the natural peptide PTR-CE1.

Furthermore, bioinformatic predictions demonstrated that the proline residue in PTR-CE1 induces a helix–kink–helix motif in its three-dimensional model. This structural alteration is likely responsible for the lack of antimicrobial effects, as several studies have reported that such kinks reduce the affinity between AMPs and bacterial membranes, leading to a loss of antimicrobial activity [45–48].

Conversely, numerous studies indicate that the formation of a continuous α-helix is strongly correlated with bioactivity of AMPs [49–52]. To test this hypothesis, we designed two peptide analogs using PTR-CE1 as a scaffold. In silico results showed that both analogs, PTR-CE1a and PTR-CE1b, form a continuous α-helix in their 3D models. Furthermore,

in silico CAMPR3 predictions yielded values close to 1, indicating that the designed peptides are likely antimicrobial. HemoPI-2 values were slightly higher than those for PTR-CE1, suggesting low hemolytic activity (Table 3) [53]. Antimicrobial assays successfully confirmed the bioactivity of these peptide analogs. PTR-CE1a displayed broad-spectrum activity against all tested microorganisms, including ampicillin-resistant isolates, while PTR-CE1b was active against the same microorganisms except for *S. aureus*.

A clear difference in potency was observed between the two peptides. The MIC of PTR-CE1a ranged from 3.02 to 12.06 μM, whereas the MIC of PTR-CE1b ranged from 106.5 to 212.99 μM, making PTR-CE1a as potent as commercial antimicrobial drugs and several designed peptides from amphibians [5,39,41,54,55]. This difference in MIC values is probably due to the higher net charge of PTR-CE1a (+7 vs. +4). These findings align with several studies demonstrating that peptides with increased cationicity exhibit enhanced antimicrobial effects compared to the original parent peptide [39,55,56].

Many frog-derived AMPs target the bacterial membrane [27,28]. Given the cationic and hydrophobic nature of PTR-CE1a and PTR-CE1b, these peptides likely inhibit pathogens via membranolytic effects. Indeed, molecular docking results showed that both peptide analogs interacted with and were embedded within a mimetic bacterial membrane, suggesting potential membrane damage.

Although these analogs show antimicrobial activity, their toxicity constitutes a major barrier to further development as therapeutic candidates. Unlike PTR-CE1, PTR-CE1a showed potent antimicrobial effects but significant hemolytic activity at the minimum inhibitory concentrations. In contrast, PTR-CEb showed lower hemolytic activity than PTR-CEa but also weaker antimicrobial activity. The ratio between the MIC and hemolytic activity is known as the selectivity index (SI), and an SI greater than 10 is generally recommended for therapeutic potential [57]. Therefore, these analogs are far from being ideal candidates for therapeutic use [58]. Nevertheless, our results demonstrate that generating analogs is a valuable strategy for understanding the physicochemical parameters and structural features required for antimicrobial activity, which can sometimes yield promising molecules with SI higher than 140 [59,60].

In summary, a novel peptide characterized from *C. ecuatoriana* that lacked antimicrobial activity was used as a template to design peptide analogs with potent antimicrobial activity. Their activity and significant toxicity are primarily attributed to their alpha-helical structure, increased hydrophobicity, and cationicity. Further design strategies are required to reduce toxicity. Therefore, our study highlights that nature-based resources represent an important source of peptides with the potential for the development of bio-inspired drugs for biomedical or biotechnological applications.

4. Materials and Methods

4.1. Collection of Callimedusa ecuatoriana Skin Secretions

One adult specimen collected from Cordillera del Cóndor, Morona Santiago Province, and two captive-born subadult specimens were provided in 2019 by Centro Jambatu for Amphibian Research and Conservation (Ecuador). Briefly, cutaneous secretions were obtained through gentle non-invasive massages to stimulate the release of skin defensive exudates from the skin granular glands. Thereafter, the secretions were collected using distilled water, immediately frozen at −80° C, lyophilized in a VirTis Benchtop Pro Freeze Dryer (Sp Scientific, Warminster, PA, USA), and stored at −20 °C [61]. Following the procedure, all specimens were returned to their terrariums without apparent harm after the process.

4.2. "Shotgun" Cloning of the Novel Peptide Precursor from C. ecuatoriana Skin Secretion-Derived cDNA Library

The poly-adenylated (poly A) mRNA from *C. ecuatoriana* skin secretion was obtained from 5 mg of lyophilized secretion dissolved in 1 mL of lysis/binding buffer using Dynabeads® mRNA DIRECT™ kit (Dynal Biotec, Merseyside, UK). The isolated mRNA was reverse transcribed to build a cDNA library using GoScript™ Reverse Transcription System and 3′CDS primer (5′-AAGCAGTGGTATCAACGCAGAGTAC T30VN-3′; V = A + C + G, N = A + T + C + G) (20 µM). Then, 3′-RACE PCR was performed to obtain *C. ecuatoriana* precursor peptide sequences using forward primer (5′-GACCAAAGATGTCWTTCTTGAAGAAAT-3′), designed from a highly conserved N-terminal opioid peptide of *Agalychnis dacnicolor* (GenBank AJ005443.1), and reverse Nested Universal Primer (NUP, 5′-AAGCAGTGGTATCAACGCAGAGT-3′). PCR products were analyzed by 2% agarose gel electrophoresis and purified using the PureLink™ PCR Purification Kit system (Invitrogen™, Carlsbad, CA, USA). The concentration and purity of DNA were verified with a Thermo Scientific™ NanoDrop™ One Microvolume UV-VIS spectrophotometer (Thermofisher, Waltham, MA, USA) and cloned using a pGEM®-T Easy vector system (Promega Corporation, Southampton, UK). Finally, the nucleotide sequence of encoded biosynthetic precursors of antimicrobial peptides was obtained by Sanger sequencing (Universidad de las Americas, Laboratory Services, Quito, EC, Ecuador).

4.3. Identification of the Novel Peptide from C. ecuatoriana Skin Secretion

The nucleotide sequences were analyzed and translated into amino acid sequences through MEGA 11 [62]. The basic local alignment was performed in BLAST/n and BLAST/p of the National Center for Biotechnology Information (NCBI) [63].

4.4. Computer-Aided Peptide Design, In Silico Predictions, and Molecular Docking

PTR-CE1 (PTR-CE1) was used as a template to design two analog peptides with enhanced antimicrobial activity. This design was supported by predictors of in silico bioactivity and toxicity. CAMPR3 was used to screen the antimicrobial effect, and HemoPI-2 to evaluate the hemolytic activity [53,64]. Additionally, the secondary structure prediction was carried out in the Self-Optimized Prediction Method from Alignment (SOPMA, https://npsa-pbil.ibcp.fr/cgi-bin/npsa_automat.pl?page=/NPSA/npsa_sopma.html, accessed on 15 January 2024) [65], and the helical wheel model of the peptides was performed using HeliQuest V2 [66]. This last tool and the Bachem Peptide Calculator were used to obtain physicochemical properties, while the theoretical mass was calculated on Peptide Mass Calculator V3.2 [67]. Finally, the three-dimensional structure of PTR-CE1 and its analogs was obtained using the I-TASSER server [68] and visualized by Pymol V3.1 [69].

Docking analysis was performed to explore the possible membranolytic effect of the peptide analogs. A bacterial membrane, composed of POPG (1-palmitoyl-2-oleoyl-sn-glycero-3-phosphoglycerol) and POPE (1-palmitoyl-2-oleoyl-sn-glycero-3-phosphoethanolamine) lipids in a ratio of 3:1, was constructed using the CHARMM-gui server V3.8 [70]. The peptide structure obtained in the previous step was used. Finally, the software Autodock Vina V1.2.X was employed in molecular docking [71]. The interaction energy between the peptide and membrane was expressed as affinity (kcal/mol).

4.5. Solid-Phase Peptide Synthesis (SPPS)

PTR-CE1 and two analogs were chemically synthesized using an automatic microwave peptide synthesizer (CEM Corporation, Matthews, NC, USA), with the solid-phase Fmoc (9-fluorenyl-methoxycarbonite) strategy. Cl-TCP (Cl) ProTide Resin (CEM, USA) was used to synthesize the acidic PTR-CE1 and Fmoc Rink Amide resin (LL) (CEM, USA) for synthesizing their analogs containing a C-terminal amidated. *N*,*N*′-dimethylformamide (DMF) was

the main solvent, and 20% piperidine was used as the deprotection reagent, while Oxyma 1M and *N*,*N*′-diisopropylcarbodiimide (DIC) 1M were used as activators in the coupling process. To cleave the resin–peptide bond, the synthesized product was incubated in the microwave system at 38 °C for 30 min with a cleavage cocktail of trifluoroacetic acid (TFA), triisopropyl silane (TIPS), 3,6-dioxa-1,8-octanedithiol (DODT), and water (92.5/2.5/2.5/2.5 $v/v/v/v$). Synthetic peptides were collected and washed after overnight precipitation using cold diethyl ether and centrifugation (5000 rpm for 15 min). Subsequently, these products were freeze-dried using a Virtis BenchTop Pro (SP Scientific) in vacuum conditions at −80 °C and stored at −20 °C. The peptide identity was confirmed by AXIMA Confidence MALDI TOF MS (Shimadzu, Columbia, MD, USA) in positive detection mode using α-Cyano-4-hydroxycinnamic acid (CHCA) as a matrix (10 mg/mL). Finally, the purity was analyzed by reverse-phase high-performance liquid chromatography (RP-HPLC) applying a linear gradient of 10% buffer (0.05% TFA, 99.95% water) to 100% buffer (99.95% CAN, 0.05% TFA) for 240 min at a 1 mL/min flow rate, with a four-pump chromatograph (Waters, Milford, MA, USA) coupled to a C_{18} Jupiter column (250 × 4.6 mm, 300 Å, 5 µm) and a UV–VIS detector at 214 nm [37,43].

4.6. Minimum Inhibitory Concentration (MIC), Minimum Bactericidal Concentration (MBC), and Minimum Fungicidal Concentration (MFC)

The minimum inhibitory concentration (MIC), minimum bactericidal concentration (MBC), and minimum fungicidal concentration (MFC) of the synthetic peptides against *Escherichia coli* ATCC 25922, *Staphylococcus aureus* ATCC 25923, *Bacillus subtilis* (ampicillin-resistant), *Klebsiella pneumoniae* (ampicillin-resistant), *Pseudomonas aeruginosa* (ampicillin-resistant), and *Candida albicans* ATCC 10231 were determined according to the protocol of Proaño-Bolaños et al. [43]. The microorganisms were cultured in Mueller–Hinton broth (MHB) to reach log phase growth (10^8 CFU/mL for bacteria and 10^6 CFU/mL for yeast), and sterile MHB was used to dilute the bacterial culture concentration to 10^6 CFU/mL. Serial dilutions of peptides (1, 2, 4, 8, 16, 32, 64, 128, 256, 512 × 10^2 mg/L) were prepared in DMSO. Then, 2 µL of peptide dilutions was mixed with 198 µL of each microorganism suspension in a 96-well microplate. MHB sterile and DMSO instead of the synthetic peptide were used as controls. Five replicates of each concentration and control were performed, and the assay was repeated three times. The microplates were incubated at 37 °C for 18 h. MIC was determined by measuring the microorganism growth at 600 nm using a GloMax® microplate reader (Promega Corporation, Madison, WI, USA). MBC and MFC were registered considering the lowest concentration without any microorganism growth after 10 µL of each concentration was cultured on Muller–Hinton Agar (MHA) and incubated overnight at 37 °C.

4.7. Hemolytic Activity

The hemolytic activity of the peptides against human red blood cell was evaluated using a 4% (v/v) suspension of erythrocytes in sterile phosphate-buffered saline (PBS) 1X. Later, 200 µL of this solution was incubated with 200 µL of serial peptide dilution (1, 2, 4, 8, 16, 32, 64, 128, 256, 512 mg/L) at 37 °C for 2 h. PBS instead of peptide was used as a negative control, and a PBS solution with Triton X-100 (2% v/v) was added as a positive control. Subsequently, the samples were centrifuged at 1000× g for 5 min, and the supernatant was transferred to 96-well microplates. Lysis of blood cells was quantified in a GloMax® plate reader (Promega, USA) at 560 nm. The percentage of hemolysis was calculated as follows:

% Hemolysis = (A − A0)/(Ax − A0) × 100%, where A = OD for the sample, Ax = OD for the positive control, and A0 = OD for the negative control [72].

Author Contributions: Conceptualization, C.P.-B.; sample collection, A.T.-V., C.P.-B. and S.B.-J.; data acquisition, S.B.-J., S.B.-P., N.E.d.l.M.-S. and G.M.-M.; writing—original draft preparation, S.B.-J. and N.E.d.l.M.-S.; data interpretation, J.R.A. and C.P.-B.; writing—critical review and editing, S.B.-P., J.R.A. and C.P.-B. All authors have read and agreed to the published version of the manuscript.

Funding: This research was funded by Ministerio del Ambiente, Agua y Transición Ecológica de Ecuador (MAATE), and Universidad Regional Amazónica Ikiam.

Institutional Review Board Statement: The study was approved by the Institutional Review Board of Universidad Regional Amazónica Ikiam for studies involving animals (DI-DBM-PA002) 26 February 2021.

Informed Consent Statement: Not applicable.

Data Availability Statement: The original contributions presented in this study are included in the article.

Acknowledgments: The collection of frogs in Ecuador was carried out under permits of the Ministerio del Ambiente of Ecuador (currently Ministerio de Ambiente Agua y Transición Ecológica—MAATE) 001-13 IC-FAU-DNB/MA, 003-11 IC-FAU-DNB/MA, and 005-15 IC-FAU-DNB/MA (issued to the Centro Jambatu de Investigación y Conservación de Anfibios). The breeding of frogs in laboratory conditions was carried out with a patent from MAATE. Sample collection and genetic analysis were carried out under the framework contracts for access to genetic resources between MAE or MAATE and Ikiam University, number: MAE-DNB-CM-2016-0051 and MAAE-DBI-CM-2021-0170. Finally, we are grateful for the kind donation of bacterial and fungal strains by Sonia Zapata (USFQ), Jorge Reyes (INSPI), and Universidad Técnica del Norte (UTN). S.B.P. would like to thank the São Paulo Research Foundation (FAPESP, 22/02936-2). During the preparation of this manuscript, the authors used Deepseek-V3.1 for the purpose of grammar correction. The authors have reviewed and edited the output and take full responsibility for the content of this publication.

Conflicts of Interest: The authors declare no conflicts of interest.

References

1. Minarini, L.A.D.R.; Andrade, L.N.D.; De Gregorio, E.; Grosso, F.; Naas, T.; Zarrilli, R.; Camargo, I.L.B.C. Editorial: Antimicrobial Resistance as a Global Public Health Problem: How Can We Address It? *Front. Public Health* **2020**, *8*, 612844. [CrossRef]
2. O'Neill, J. *Tacking Drug Resistant Infections Globally: Final Report and Recommendations*; Government of the United Kingdom: London, UK, 2016.
3. Bucataru, C.; Ciobanasu, C. Antimicrobial Peptides: Opportunities and Challenges in Overcoming Resistance. *Microbiol. Res.* **2024**, *286*, 127822. [CrossRef]
4. Demori, I.; El Rashed, Z.; Corradino, V.; Catalano, A.; Rovegno, L.; Queirolo, L.; Salvidio, S.; Biggi, E.; Zanotti-Russo, M.; Canesi, L.; et al. Peptides for Skin Protection and Healing in Amphibians. *Molecules* **2019**, *24*, 347. [CrossRef]
5. Xu, X.; Lai, R. The Chemistry and Biological Activities of Peptides from Amphibian Skin Secretions. *Chem. Rev.* **2015**, *115*, 1760–1846. [CrossRef] [PubMed]
6. Modi, A.; Uniyal, A.; Akhilesh Tiwari, V.; Chouhan, D.; Agrawal, S.; Ummadisetty, O.; Tiwari, V. Dermorphin [D-Arg2, Lys4] (1–4) Amide Attenuates Burn Pain by Inhibiting TRPV1/NR2B Mediated Neuroinflammatory Signalling. *Mol. Neurobiol.* **2025**, *62*, 12668–12687. [CrossRef] [PubMed]
7. Pantic, J.M.; Jovanovic, I.P.; Radosavljevic, G.D.; Arsenijevic, N.N.; Conlon, J.M.; Lukic, M.L. The Potential of Frog Skin-Derived Peptides for Development into Therapeutically-Valuable Immunomodulatory Agents. *Molecules* **2017**, *22*, 2071. [CrossRef]
8. Conlon, J.M.; Owolabi, B.O.; Flatt, P.R.; Abdel-Wahab, Y.H.A. Amphibian Host-Defense Peptides with Potential for Type 2 Diabetes Therapy—An Updated Review. *Peptides* **2024**, *175*, 171180. [CrossRef] [PubMed]
9. Tolos, A.M.; Moisa, C.; Dochia, M.; Popa, C.; Copolovici, L.; Copolovici, D.M. Anticancer Potential of Antimicrobial Peptides: Focus on Buforins. *Polymers* **2024**, *16*, 728. [CrossRef]
10. Chen, D.; Zhou, X.; Chen, X.; Huang, L.; Xi, X.; Ma, C.; Zhou, M.; Wang, L.; Chen, T. Evaluating the Bioactivity of a Novel Antimicrobial and Anticancer Peptide, Dermaseptin-PS4 (Der-PS4), from the Skin Secretion of *Phyllomedusa sauvagii*. *Molecules* **2019**, *24*, 2974. [CrossRef] [PubMed]
11. Li, X.; Wang, Y.; Zou, Z.; Yang, M.; Wu, C.; Su, Y.; Tang, J.; Yang, X. OM-LV20, a Novel Peptide from Odorous Frog Skin, Accelerates Wound Healing In Vitro and In Vivo. *Chem. Biol. Drug Des.* **2018**, *91*, 126–136. [CrossRef]

12. Liu, S.; Long, Q.; Xu, Y.; Wang, J.; Xu, Z.; Wang, L.; Zhou, M.; Wu, Y.; Chen, T.; Shaw, C. Assessment of Antimicrobial and Wound Healing Effects of Brevinin-2Ta against the Bacterium *Klebsiella pneumoniae* in Dermally-Wounded Rats. *Oncotarget* **2017**, *8*, 111369–111385. [CrossRef]
13. Wang, Y.; Cao, X.; Fu, Z.; Wang, S.; Li, X.; Liu, N.; Feng, Z.; Yang, M.; Tang, J.; Yang, X. Identification and Characterization of a Novel Gene-Encoded Antioxidant Peptide Obtained from Amphibian Skin Secretions. *Nat. Prod. Res.* **2020**, *34*, 754–758. [CrossRef]
14. Udovychenko, I.; Oliynyk, D.; Dudkina, J.; Halenova, T.; Savchuk, O. Analysis of the Common Spadefoot Toad (*Pelobates fuscus*) Skin Secretions on the Presence of the Potential Hemostasis System Effectors. *Bull. Taras Shevchenko Natl. Univ. Kyiv. Ser. Biol.* **2019**, *77*, 38–44. [CrossRef]
15. Chen, X.; Liu, S.; Fang, J.; Zheng, S.; Wang, Z.; Jiao, Y.; Xia, P.; Wu, H.; Ma, Z.; Hao, L. Peptides Isolated from Amphibian Skin Secretions with Emphasis on Antimicrobial Peptides. *Toxins* **2022**, *14*, 722. [CrossRef]
16. Prates, M.V.; Sforça, M.L.; Regis, W.C.B.; Leite, J.R.S.A.; Silva, L.P.; Pertinhez, T.A.; Araújo, A.L.T.; Azevedo, R.B.; Spisni, A.; Bloch, C. The NMR-Derived Solution Structure of a New Cationic Antimicrobial Peptide from the Skin Secretion of the Anuran *Hyla punctata*. *J. Biol. Chem.* **2004**, *279*, 13018–13026. [CrossRef] [PubMed]
17. Wang, G.; Li, X.; Wang, Z. APD3: The Antimicrobial Peptide Database as a Tool for Research and Education. *Nucleic Acids Res.* **2016**, *44*, D1087–D1093. [CrossRef] [PubMed]
18. Kosikowska, P.; Lesner, A. Antimicrobial Peptides (AMPs) as Drug Candidates: A Patent Review (2003–2015). *Expert. Opin. Ther. Pat.* **2016**, *26*, 689–702. [CrossRef] [PubMed]
19. Erspamer, V.; Melchiorri, P.; Falconieri Erspamer, G.; Montecucchi, P.C.; de Castiglione, R. *Phyllomedusa* Skin: A Huge Factory and Store-House of a Variety of Active Peptides. *Peptides* **1985**, *6*, 7–12. [CrossRef]
20. Ge, L.; Chen, X.; Ma, C.; Zhou, M.; Xi, X.; Wang, L.; Ding, A.; Duan, J.; Chen, T.; Shaw, C. Balteatide: A Novel Antimicrobial Decapeptide from the Skin Secretion of the Purple-Sided Leaf Frog. *Phyllomedusa baltea. Sci. World J.* **2014**, *2014*, 176214. [CrossRef]
21. Shi, D.; Xi, X.; Wang, L.; Gao, Y.; Ma, C.; Chen, H.; Zhou, M.; Chen, T.; Shaw, C. Baltikinin: A New Myotropic Tryptophyllin-3 Peptide Isolated from the Skin Secretion of the Purple-Sided Leaf Frog, *Phyllomedusa baltea*. *Toxins* **2016**, *8*, 213. [CrossRef]
22. Zhu, H.; Ding, X.; Li, W.; Lu, T.; Ma, C.; Xi, X.; Wang, L.; Zhou, M.; Burden, R.; Chen, T. Discovery of Two Skin-Derived Dermaseptins and Design of a TAT-Fusion Analogue with Broad-Spectrum Antimicrobial Activity and Low Cytotoxicity on Healthy Cells. *PeerJ* **2018**, *2018*, e5635. [CrossRef]
23. Yin, W.; Yao, J.; Leng, X.; Ma, C.; Chen, X.; Jiang, Y.; Wang, T.; Chen, T.; Shaw, C.; Zhou, M.; et al. Enhancement of Antimicrobial Function by L/D-Lysine Substitution on a Novel Broad-Spectrum Antimicrobial Peptide, Phylloseptin-TO2: A Structure-Related Activity Research Study. *Pharmaceutics* **2024**, *16*, 1098. [CrossRef]
24. Chen, Z.; Xi, X.; Lu, Y.; Hu, H.; Dong, Z.; Ma, C.; Wang, L.; Zhou, M.; Chen, T.; Du, S.; et al. In Vitro Activities of a Novel Antimicrobial Peptide Isolated from *Phyllomedusa tomopterna*. *Microb. Pathog.* **2021**, *153*, 104795. [CrossRef]
25. Ron, S.R.; Read, M. *Phyllomedusa ecuatoriana*. Available online: https://bioweb.bio/faunaweb/amphibiaweb/FichaEspecie/Phyllomedusa%20ecuatoriana (accessed on 13 August 2025).
26. Xuan, J.; Feng, W.; Wang, J.; Wang, R.; Zhang, B.; Bo, L.; Chen, Z.S.; Yang, H.; Sun, L. Antimicrobial Peptides for Combating Drug-Resistant Bacterial Infections. *Drug Resist. Updates* **2023**, *68*, 100954. [CrossRef] [PubMed]
27. Li, X.; Zuo, S.; Wang, B.; Zhang, K.; Wang, Y. Antimicrobial Mechanisms and Clinical Application Prospects of Antimicrobial Peptides. *Molecules* **2022**, *27*, 2675. [CrossRef]
28. Zhang, R.; Xu, L.; Dong, C. Antimicrobial Peptides: An Overview of Their Structure, Function and Mechanism of Action. *Protein Pept. Lett.* **2022**, *29*, 641–650. [CrossRef] [PubMed]
29. Lazzaro, B.P.; Zasloff, M.; Rolff, J. Antimicrobial Peptides: Application Informed by Evolution. *Science* **2020**, *368*, eaau5480. [CrossRef]
30. Fjell, C.D.; Hiss, J.A.; Hancock, R.E.W.; Schneider, G. Designing Antimicrobial Peptides: Form Follows Function. *Nat. Rev. Drug Discov.* **2012**, *11*, 37–51. [CrossRef]
31. Lei, J.; Sun, L.C.; Huang, S.; Zhu, C.; Li, P.; He, J.; Mackey, V.; Coy, D.H.; He, Q.Y. The Antimicrobial Peptides and Their Potential Clinical Applications. *Am. J. Transl. Res.* **2019**, *11*, 3919. [PubMed]
32. Hancock, R.E.W.; Sahl, H.G. Antimicrobial and Host-Defense Peptides as New Anti-Infective Therapeutic Strategies. *Nat. Biotechnol.* **2006**, *24*, 1551–1557. [CrossRef]
33. Otvos, L.; Wade, J.D. Current Challenges in Peptide-Based Drug Discovery. *Front. Chem.* **2014**, *2*, 62. [CrossRef]
34. Mwangi, J.; Kamau, P.M.; Thuku, R.C.; Lai, R. Design Methods for Antimicrobial Peptides with Improved Performance. *Zool. Res.* **2023**, *44*, 1095–1114. [CrossRef]
35. Bermúdez-Puga, S.; Morán-Marcillo, G.; Espinosa de los Monteros-Silva, N.; Naranjo, R.E.; Toscano, F.; Vizuete, K.; Torres Arias, M.; Almeida, J.R.; Proaño-Bolaños, C. Inspiration from Cruzioseptin-1: Membranolytic Analogue with Improved Antibacterial Properties. *Amino Acids* **2023**, *55*, 113–124. [CrossRef]

36. Bermúdez-Puga, S.; Dias, M.; Lima Reis, I.; Freire de Oliveira, T.; Yokomizo de Almeida, S.R.; Mendes, M.A.; Moore, S.J.; Almeida, J.R.; Proaño-Bolaños, C.; Pinheiro de Souza Oliveira, R. Microscopic and Metabolomics Analysis of the Anti-*Listeria* Activity of Natural and Engineered Cruzioseptins. *Biochimie* **2024**, *225*, 168–175. [CrossRef] [PubMed]
37. Morán-Marcillo, G.; Sánchez Hinojosa, V.; de los Monteros-Silva, N.E.; Blasco-Zúñiga, A.; Rivera, M.; Naranjo, R.E.; Almeida, J.R.; Wang, L.; Zhou, M.; Chen, T.; et al. Picturins and Pictuseptins, Two Novel Antimicrobial Peptide Families from the Skin Secretions of the Chachi Treefrog, *Boana picturata*. *J. Proteom.* **2022**, *264*, 104633. [CrossRef]
38. Pál, T.; Sonnevend, Á.; Galadari, S.; Conlon, J.M. Design of Potent, Non-Toxic Antimicrobial Agents Based upon the Structure of the Frog Skin Peptide, Pseudin-2. *Regul. Pept.* **2005**, *129*, 85–91. [CrossRef] [PubMed]
39. Park, H.J.; Kang, H.K.; Park, E.; Kim, M.K.; Park, Y. Bactericidal Activities and Action Mechanism of the Novel Antimicrobial Peptide Hylin A1 and Its Analog Peptides against *Acinetobacter baumannii* Infection. *Eur. J. Pharm. Sci.* **2022**, *175*, 106205. [CrossRef]
40. Pál, T.; Abraham, B.; Sonnevend, Á.; Jumaa, P.; Conlon, J.M. Brevinin-1BYa: A Naturally Occurring Peptide from Frog Skin with Broad-Spectrum Antibacterial and Antifungal Properties. *Int. J. Antimicrob. Agents* **2006**, *27*, 525–529. [CrossRef] [PubMed]
41. Conlon, J.M.; Mechkarska, M.; Arafat, K.; Attoub, S.; Sonnevend, A. Analogues of the Frog Skin Peptide Alyteserin-2a with Enhanced Antimicrobial Activities against Gram-Negative Bacteria. *J. Pept. Sci.* **2012**, *18*, 270–275. [CrossRef]
42. Kim, J.B.; Conlon, J.M.; Iwamuro, S.; Knoop, F.C. Antimicrobial Peptides from the Skin of the Japanese Mountain Brown Frog, *Rana ornativentris*. *J. Pept. Res.* **2001**, *58*, 349–356. [CrossRef]
43. Proaño-Bolaños, C.; Zhou, M.; Wang, L.; Coloma, L.A.; Chen, T.; Shaw, C. Peptidomic Approach Identifies Cruzioseptins, a New Family of Potent Antimicrobial Peptides in the Splendid Leaf Frog, *Cruziohyla calcarifer*. *J. Proteom.* **2016**, *146*, 1–13. [CrossRef]
44. Funk, C.; Caminer, M.; Ron, S.R. High Levels of Cryptic Species Diversity Uncovered in Amazonian Frogs. *Proc. R. Soc. B Biol. Sci.* **2012**, *279*, 1806–1814. [CrossRef] [PubMed]
45. Brožek, R.; Kabelka, I.; Vácha, R. Effect of Helical Kink on Peptide Translocation across Phospholipid Membranes. *J. Phys. Chem. B* **2020**, *124*, 5940–5947. [CrossRef] [PubMed]
46. Yan, J.; Liang, X.; Liu, C.; Cheng, Y.; Zhou, L.; Wang, K.; Zhao, L. Influence of Proline Substitution on the Bioactivity of Mammalian-Derived Antimicrobial Peptide NK-2. *Probiotics Antimicrob. Proteins* **2018**, *10*, 118–127. [CrossRef]
47. Park, S.H.; Kim, H.E.; Kim, C.M.; Yun, H.J.; Choi, E.C.; Lee, B.J. Role of Proline, Cysteine and a Disulphide Bridge in the Structure and Activity of the Anti-Microbial Peptide Gaegurin 5. *Biochem. J.* **2002**, *368*, 171–182. [CrossRef]
48. Chen, G.; Miao, Y.; Ma, C.; Zhou, M.; Shi, Z.; Chen, X.; Burrows, J.F.; Xi, X.; Chen, T.; Wang, L. Brevinin-2GHK from *Sylvirana guentheri* and the Design of Truncated Analogs Exhibiting the Enhancement of Antimicrobial Activity. *Antibiotics* **2020**, *9*, 85. [CrossRef]
49. Zelezetsky, I.; Tossi, A. Alpha-Helical Antimicrobial Peptides-Using a Sequence Template to Guide Structure-Activity Relationship Studies. *Biochim. Biophys. Acta Biomembr.* **2006**, *1758*, 1436–1449. [CrossRef]
50. Eliseev, I.E.; Terterov, I.N.; Yudenko, A.N.; Shamova, O.V. Linking Sequence Patterns and Functionality of Alpha-Helical Antimicrobial Peptides. *Bioinformatics* **2019**, *35*, 2713–2717. [CrossRef]
51. Huang, Y.; Huang, J.; Chen, Y. Alpha-Helical Cationic Antimicrobial Peptides: Relationships of Structure and Function. *Protein Cell* **2010**, *1*, 143–152. [CrossRef] [PubMed]
52. Guilhaudis, L.; Cunning, T.S.; Delaney, J.J.; Ternan, N.G.; Mechkarska, M.; Attoub, S.; Conlon, J.M. Substitution of a Proline Residue in the Frog Skin Host-Defense Peptide, Figainin-2PL by D-Lysine Generates an Analog with Potent Activity against Antibiotic-Resistant ESKAPE Pathogens. *Peptides* **2025**, *192*, 171430. [CrossRef]
53. Chaudhary, K.; Kumar, R.; Singh, S.; Tuknait, A.; Gautam, A.; Mathur, D.; Anand, P.; Varshney, G.C.; Raghava, G.P.S. A Web Server and Mobile App for Computing Hemolytic Potency of Peptides. *Sci. Rep.* **2016**, *6*, 22843. [CrossRef] [PubMed]
54. Conlon, J.M.; Abraham, B.; Galadari, S.; Knoop, F.C.; Sonnevend, A.; Pál, T. Antimicrobial and Cytolytic Properties of the Frog Skin Peptide, Kassinatuerin-1 and Its L- and D-Lysine-Substituted Derivatives. *Peptides* **2005**, *26*, 2104–2110. [CrossRef]
55. Tan, Y.; Chen, X.; Ma, C.; Xi, X.; Wang, L.; Zhou, M.; Burrows, J.F.; Kwok, H.F.; Chen, T. Biological Activities of Cationicity-Enhanced and Hydrophobicity-Optimized Analogues of an Antimicrobial Peptide, Dermaseptin-PS3, from the Skin Secretion of *Phyllomedusa sauvagii*. *Toxins* **2018**, *10*, 320. [CrossRef]
56. Gong, Z.; Pei, X.; Ren, S.; Chen, X.; Wang, L.; Ma, C.; Xi, X.; Chen, T.; Shaw, C.; Zhou, M. Identification and Rational Design of a Novel Antibacterial Peptide Dermaseptin-Ac from the Skin Secretion of the Red-Eyed Tree Frog *Agalychnis callidryas*. *Antibiotics* **2020**, *9*, 243. [CrossRef]
57. Juretić, D.; Simunić, J. Design of α-Helical Antimicrobial Peptides with a High Selectivity Index. *Expert. Opin. Drug Discov.* **2019**, *14*, 1053–1063. [CrossRef]
58. Tamargo, J.; Le Heuzey, J.Y.; Mabo, P. Narrow Therapeutic Index Drugs: A Clinical Pharmacological Consideration to Flecainide. *Eur. J. Clin. Pharmacol.* **2015**, *71*, 549–567. [CrossRef] [PubMed]
59. Azuma, E.; Choda, N.; Odaki, M.; Yano, Y.; Matsuzaki, K. Improvement of Therapeutic Index by the Combination of Enhanced Peptide Cationicity and Proline Introduction. *ACS Infect. Dis.* **2020**, *6*, 2271–2278. [CrossRef]

60. Di, Y.P.; Lin, Q.; Chen, C.; Montelaro, R.C.; Doi, Y.; Deslouches, B. Enhanced Therapeutic Index of an Antimicrobial Peptide in Mice by Increasing Safety and Activity against Multidrug-Resistant Bacteria. *Health Med.* **2020**, *6*, eaay6817. [CrossRef]
61. Clark, V.C. Collecting Arthropod and Amphibian Secretions for Chemical Analysis. In *Behavioral Chemical Ecology*; Zhiang, W., Liu, H., Eds.; Nova Science Publishers, Inc.: Hauppauge, NY, USA, 2009; ISBN 978-1-60741-099-7.
62. Tamura, K.; Stecher, G.; Kumar, S. MEGA11: Molecular Evolutionary Genetics Analysis Version 11. *Mol. Biol. Evol.* **2021**, *38*, 3022–3027. [CrossRef]
63. Altschul, S.F.; Gish, W.; Miller, W.; Myers, E.W.; Lipman, D.J. Basic Local Alignment Search Tool. *J. Mol. Biol.* **1990**, *215*, 403–410. [CrossRef] [PubMed]
64. Waghu, F.H.; Barai, R.S.; Gurung, P.; Idicula-Thomas, S. CAMPR3: A Database on Sequences, Structures and Signatures of Antimicrobial Peptides. *Nucleic Acids Res.* **2016**, *44*, D1094–D1097. [CrossRef] [PubMed]
65. Geourjon, C.; Deléage, G. Sopma: Significant Improvements in Protein Secondary Structure Prediction by Consensus Prediction from Multiple Alignments. *Bioinformatics* **1995**, *11*, 681–684. [CrossRef] [PubMed]
66. Gautier, R.; Douguet, D.; Antonny, B.; Drin, G. HELIQUEST: A Web Server to Screen Sequences with Specific α-Helical Properties. *Bioinformatics* **2008**, *24*, 2101–2102. [CrossRef]
67. Rozenski, J. *Peptide Mass Calculator, v3.2*; Rega Institute for Medical Research: Leuven, Belgium, 1999.
68. Yang, J.; Zhang, Y. I-TASSER Server: New Development for Protein Structure and Function Predictions. *Nucleic Acids Res.* **2015**, *43*, W174–W181. [CrossRef]
69. Schrödinger, L. *The PyMol Molecular Graphics System*, Versión 1.8; Schrdinger, LLC: New York, NY, USA, 2015.
70. Feng, S.; Park, S.; Choi, Y.K.; Im, W. CHARMM-GUI Membrane Builder: Past, Current, and Future Developments and Applications. *J. Chem. Theory Comput.* **2023**, *19*, 2161–2185. [CrossRef]
71. Trott, O.; Olson, A.J. AutoDock Vina: Improving the Speed and Accuracy of Docking with a New Scoring Function, Efficient Optimization, and Multithreading. *J. Comput. Chem.* **2010**, *31*, 455–461. [CrossRef]
72. Proaño-Bolaños, C.; Blasco-Zúñiga, A.; Almeida, J.R.; Wang, L.; Llumiquinga, M.A.; Rivera, M.; Zhou, M.; Chen, T.; Shaw, C. Unravelling the Skin Secretion Peptides of the Gliding Leaf Frog, *Agalychnis spurrelli* (Hylidae). *Biomolecules* **2019**, *9*, 667. [CrossRef] [PubMed]

Disclaimer/Publisher's Note: The statements, opinions and data contained in all publications are solely those of the individual author(s) and contributor(s) and not of MDPI and/or the editor(s). MDPI and/or the editor(s) disclaim responsibility for any injury to people or property resulting from any ideas, methods, instructions or products referred to in the content.